

# Phase Frustration-Induced Spatial Lattice Symmetry

July 4, 2025

## Contents

<b>1</b>	<b>The Model</b>	<b>1</b>
<b>2</b>	<b>Phase frustration-induced crystallization</b>	<b>1</b>
2.1	Key properties	1
<b>3</b>	<b>Mechanism</b>	<b>6</b>
3.1	Hydrodynamics	6
3.2	Abstract phase oscillator model	7

## 1 The Model

Particles have a spatial position  $\mathbf{r}_i = (x_i, y_i)$  and an internal phase  $\theta_i$  which evolve according to equations:

$$\dot{\mathbf{r}}_i = v \mathbf{p}(\theta_i) , \quad (1a)$$

$$\dot{\theta}_i = \omega_i + \frac{K}{|A_i|} \sum_{j \in A_i} [\sin(\theta_j - \theta_i + \alpha) - \sin \alpha] , \quad (1b)$$

for  $i = 1, 2, \dots, N$ . Here in Eq. (1a),  $\mathbf{p}(\theta) = (\cos \theta, \sin \theta)$ , which means each particle rotates with a constant speed  $v$  in the direction of its instantaneous phase  $\theta_i(t)$ . The particles are treated as point-like with no direct spatial interactions, consistent with classical models of chiral self-propelled particles [1–3, 7, 8]. As per Eq. (1b), the mean runs over neighbors within a coupling radius  $d_0$  around particle  $i$ :

$$A_i(t) = \{j \mid |\mathbf{r}_i(t) - \mathbf{r}_j(t)| \leq d_0\} , \quad (2)$$

$K (\geq 0)$  is the coupling strength, and  $\{\omega_i\}$  are the natural frequencies distributed according to a given frequency distribution  $g(\omega)$ . This means that a particle will rotate with the angular velocity  $|\omega_i|$  in the absence of mutual coupling ( $K = 0$ ), and the sign of  $\omega_i$  represents the direction of rotation, namely, the tribute of the chirality of the  $i$ -th particle. A positive (negative) chirality ( $\omega$ ) describes the counterclockwise (clockwise) rotations of the particle in space.

Additionally,  $\alpha$  is the phase frustration between two neighboring particles. When  $\alpha_0 = 0$ , the dynamics reduces to the normal chiral model [4]. The counter term  $-\sin \alpha$  is introduced to ensure that frustration only interferes with the phase coupling without changing the sign of effective frequency.

## 2 Phase frustration-induced crystallization

### 2.1 Key properties

1. What does the lattice structure look like?
2. **Done** What is each cell composed of?

3. What is the unit cell structure, and what is the spatial arrangement of the unit cells?
4. What is the internal dynamics within a cell? Besides triangular, what other spatial structures exist?
5. What determines the length (periodicity)? (Interaction distance?) In which regions of frustration does it appear? (And what are the corresponding coupling conditions and natural frequency distributions?)

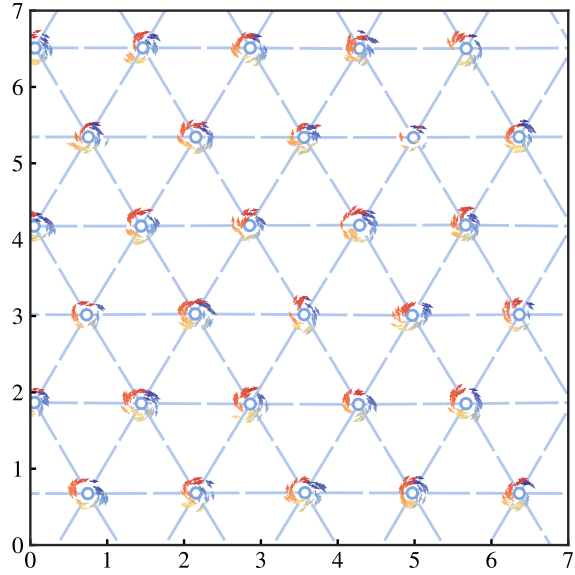


Figure 1: Snapshots of achiral system ( $\omega_{\min} = 0$  and  $\Delta\omega = 0$ ) at  $t = 80$  with  $N = 1000$ ,  $K = 20$ ,  $\alpha = 0.6\pi$ ,  $\omega_{\min} = 0$ , and  $\Delta\omega = 1$ .

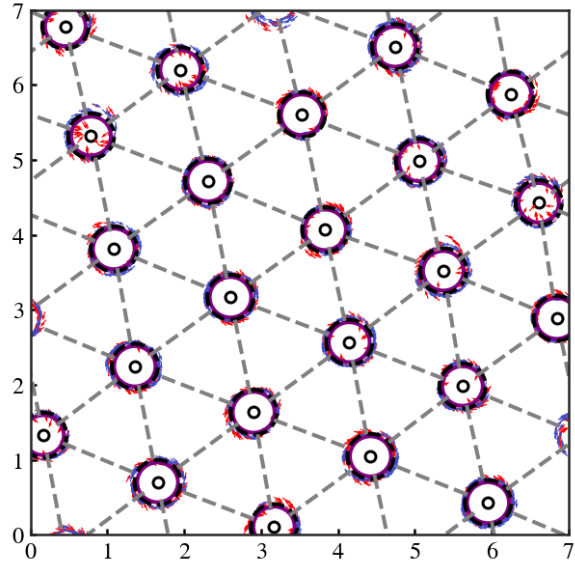


Figure 2: Snapshots of system at  $t = 80$  with  $N = 1000$ ,  $K = 10.5$ ,  $d_0 = 1.07$ ,  $\alpha = 0.6\pi$ ,  $\omega_{\min} = 0$ , and  $\Delta\omega = 1$ .

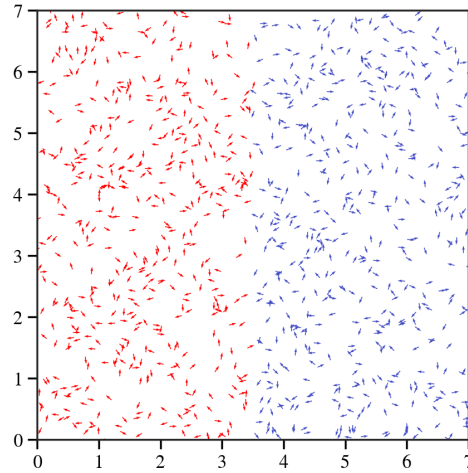


Figure 3: Initial conditions of half on each side.

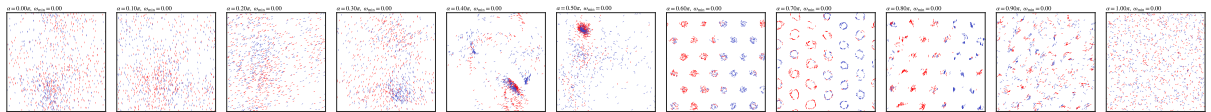


Figure 4: Snapshot of the system at  $t = 80$  with  $N = 1000$ ,  $K = 20$ ,  $\omega_{\min} = 0$ ,  $\Delta\omega = 1$  and initial conditions of half on each side.

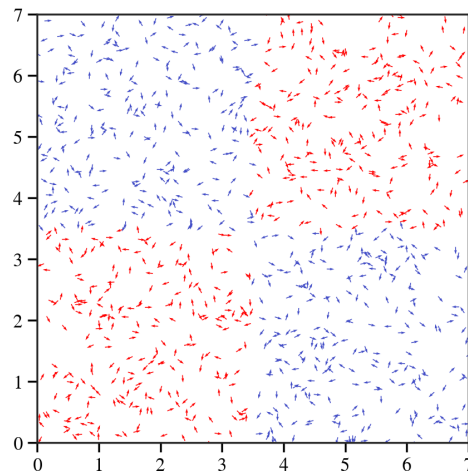


Figure 5: Initial conditions of chessboard pattern.

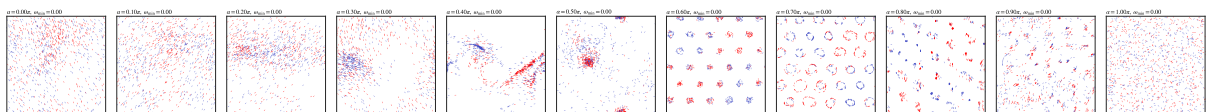


Figure 6: Snapshot of the system at  $t = 80$  with  $N = 1000$ ,  $K = 20$ ,  $\omega_{\min} = 0$ ,  $\Delta\omega = 1$  and initial conditions of chessboard pattern.

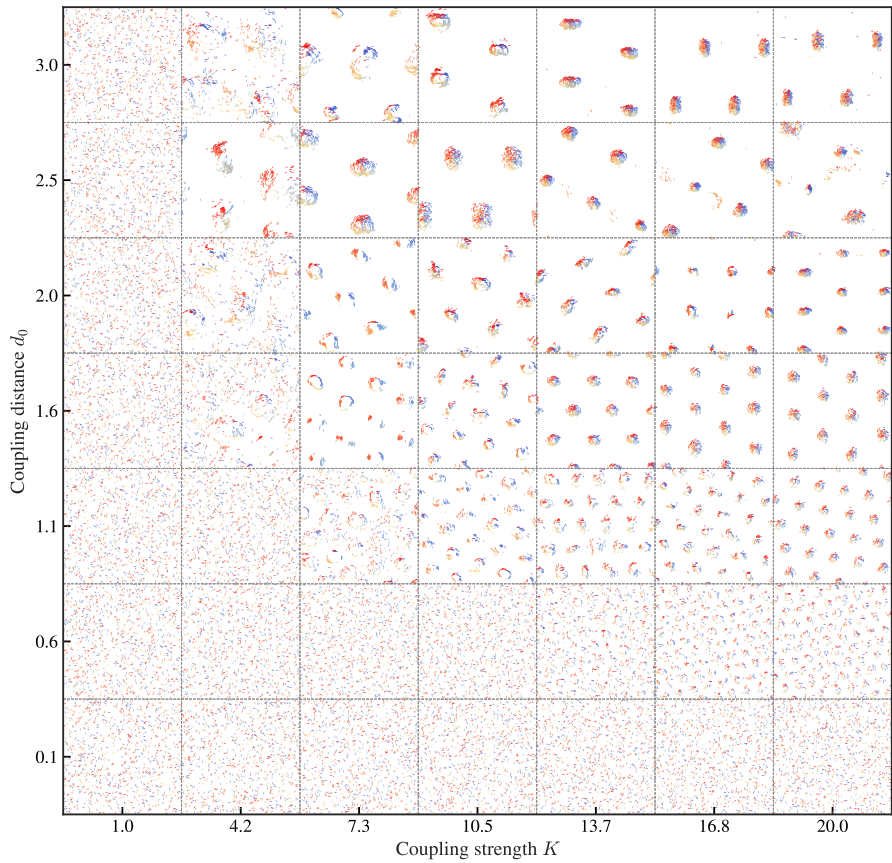


Figure 7: Snapshots of achiral system ( $\omega_{\min} = 0$  and  $\Delta\omega = 0$ ) at different coupling strengths  $K$  and radius  $d_0$  for  $\alpha = 0.6\pi$ . 固定阻挫为  $0.6\pi$ , 不同的耦合强度  $K$  和半径  $d_0$  下的非手性粒子系统快照。粒子颜色根据其瞬时相位  $\theta_i$  着色。随着两个耦合参数的增加, 粒子在空间中逐渐形成三角晶格结构且尺寸和彼此距离不断增加。

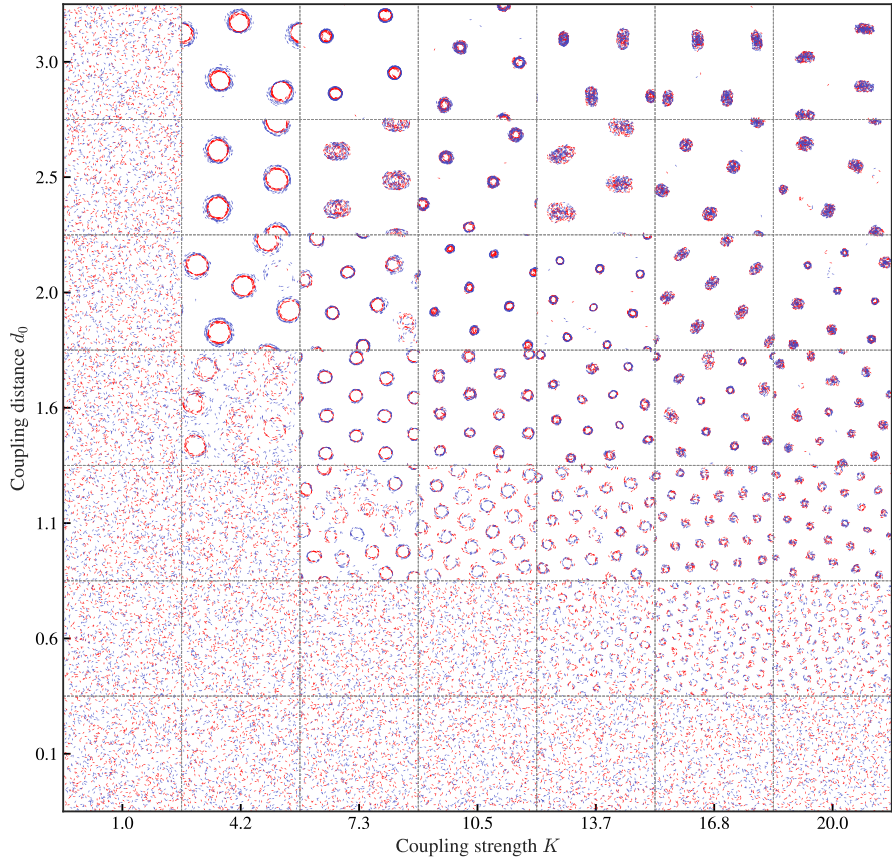


Figure 8: Snapshots of system at different coupling strengths  $K$  and radius  $d_0$  with  $N = 1000$ ,  $K = 20$ ,  $\alpha = 0.6\pi$ ,  $\omega_{\min} = 0$ , and  $\Delta\omega = 1$ . 固定阻挫为  $0.6\pi$ , 不同的耦合强度  $K$  和半径  $d_0$  下的手性粒子系统快照。粒子颜色根据其瞬时相位  $\theta_i$  着色。随着两个耦合参数的增加, 粒子在空间中逐渐形成三角晶格结构且尺寸和彼此距离不断增加。

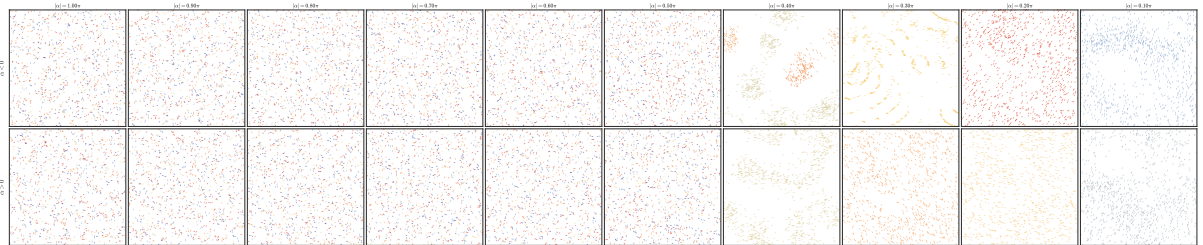


Figure 9: Snapshot of the system without counter term  $-\sin\alpha$  at  $t = 80$  with  $N = 1000$ ,  $K = 20$ ,  $\omega_{\min} = 0.1$  and  $\Delta\omega = 1$ . The particles are colored according to their instantaneous phase  $\theta_i$ . There is no triangular lattice structure, and the particles are randomly distributed in space. 系统终态的快照, 粒子颜色根据其瞬时相位  $\theta_i$  着色。空间排列没有三角晶格结构, 粒子在空间中随机分布。

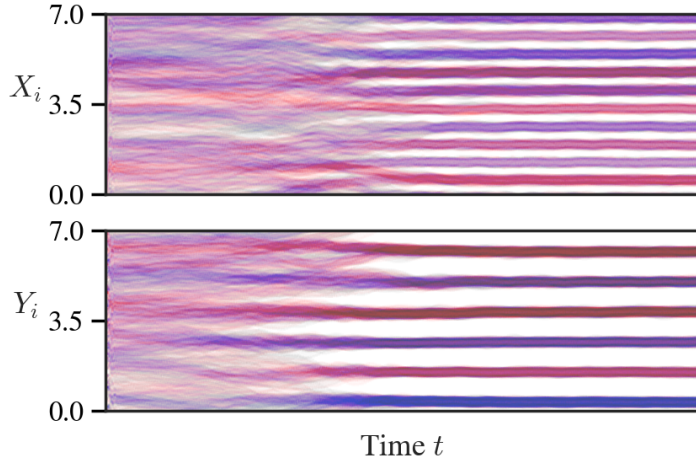


Figure 10: 瞬时旋转中心随时间变化的散点图。其中  $N = 1000$ ,  $K = 20$ ,  $\alpha = 0.6\pi$ ,  $\omega_{\min} = 0.1$ 。随时间演化，粒子晶格大体呈现红蓝交错分布的趋势。

陆羿辰：从旋转中心的散点图确实能看出一些红蓝交替出现的现象，原因暂时不明（也可能和画散点图时图层的排序有关，可以尝试改变一下图层的顺序）

陆羿辰：调整完图层之后色调发生了改变，目前猜测应该不是类似棋盘格的分布

### 3 Mechanism

#### 3.1 Hydrodynamics

Here, we develop a continuum theory for the self-propelled particles with phase frustration, following the approach in [2, 3]. We start with the Eqs. (1) but replace the finite range alignment interaction by a pseudopotential (' $\delta'$ -interaction), which is justified if the interaction is short ranged enough, such that the shape of the associated interaction potential is irrelevant to the many particle dynamics. Additionally, for simplicity of analysis, we consider achiral systems ( $\omega_i = 0$ ). Then

$$\dot{\mathbf{r}}_i = v \mathbf{p}(\theta_i) , \quad (3a)$$

$$\dot{\theta}_i = \frac{K}{|A_i|} \sum_{j=1}^N \delta(\mathbf{r}_j - \mathbf{r}_i) [\sin(\theta_j - \theta_i + \alpha) - \sin \alpha] . \quad (3b)$$

In the thermodynamic limit  $N \rightarrow \infty$ , the agent-based model gives rise to the following continuum form:

$$\frac{\partial}{\partial t} f(\mathbf{r}, \theta, t) = -\nabla \cdot (f \mathbf{v}_r) - \frac{\partial}{\partial \theta} (f v_\theta) , \quad (4)$$

where  $f(\mathbf{r}, \theta, t)$  is the probability density of particles at position  $\mathbf{r}$  and orientation  $\theta$  at time  $t$ , and  $\mathbf{v}_r$  and  $v_\theta$  are the velocity fields in the position and orientation space, respectively. The velocity fields are given by

$$\mathbf{v}_r(\mathbf{r}, \theta, t) = v \mathbf{p}(\theta) \quad (5a)$$

$$v_\theta(\mathbf{r}, \theta, t) = -\sin \alpha + K \int d\theta' f(\mathbf{r}, \theta', t) \sin(\theta' - \theta + \alpha) . \quad (5b)$$

By substituting Eqs. (5) into Eq. (4), we obtain

### 3.2 Abstract phase oscillator model

Let us consider a decoupled phase-oscillator system

$$\dot{\theta}_i = \omega_i - K \sin \alpha + \frac{K}{N} \sum_{j=1}^N \sin (\theta_j - \theta_i + \alpha) . \quad (6)$$

To quantify the phase coherence of the system, it is convenient to define the generalized complex-valued order parameters, i.e.,

$$Z(t) = R(t) e^{i\psi(t)} = \frac{1}{N} \sum_{j=1}^N e^{i\theta_j(t)}, \quad (7)$$

where  $n = 1, 2, \dots, N$ , and  $r(t)$ ,  $\psi(t)$  are the amplitudes and arguments of the order parameter. Our starting point is to analyze the critical point for the coherence of the order parameter. In the thermodynamic limit  $N \rightarrow \infty$ , the state of the system in Eq. (6) can be characterized by the single-oscillator distribution  $\rho(\theta, \omega, t)$ , which satisfies the continuity equation

$$\frac{\partial \rho}{\partial t} + \frac{\partial(\rho v)}{\partial \theta} = 0, \quad (8)$$

where  $\rho(\theta, \omega, t)$  accounts for the fraction of oscillators with phase  $\theta$  lying in the interval  $(\theta, \theta + d\theta)$  at fixed frequency  $\omega$  and time  $t$ , it satisfies the normalization condition

$$\int_0^{2\pi} \rho(\theta, \omega, t) d\theta = 1. \quad (9)$$

Here,  $v(\theta, \omega, t)$  is the velocity field, given by

$$v(\theta, \omega, t) = K \int_{-\infty}^{+\infty} \int_0^{2\pi} \sin(\theta' - \theta + \alpha) \rho d\theta' d\omega' + \omega - K \sin \alpha. \quad (10)$$

Correspondingly, the order parameter defined in Eq. (7) in the thermodynamic limit reads

$$Z(t) = \int_{-\infty}^{+\infty} g(\omega) d\omega \int_0^{2\pi} e^{i\theta} \rho(\theta, \omega, t) d\theta, \quad (11)$$

then  $v(\theta, \omega, t)$  simplifies to

$$v(\theta, \omega, t) = \omega - K \sin \alpha + \text{Im} [H(t) e^{-i\theta}], \quad (12)$$

with the mean-field being

$$H(t) = K Z(t) e^{i\alpha}. \quad (13)$$

Since the distribution  $\rho(\theta, \omega, t)$  is  $2\pi$ -periodic in  $\theta$ , we can expand it in Fourier series as

$$\rho(\theta, \omega, t) = \frac{1}{2\pi} \sum_{n=-\infty}^{+\infty} a_n(\omega, t) e^{in\theta}, \quad (14)$$

where  $a_n(\omega, t)$  is the  $n$ -th Fourier coefficient. In particular, we have  $a_0(\omega, t) = 1$  owing to the normalization condition in Eq. (9) and  $a_{-n}(\omega, t) = a_n^*(\omega, t)$ , where  $*$  denotes the complex conjugate.

According to the Ott-Antonsen ansatz [5, 6], it states that the  $n$ -th Fourier coefficient  $a_n(\omega, t)$  can be expressed in terms of the first-order coefficient, i.e.,  $a_n(\omega, t) = a^n(\omega, t)$ . In this regard, the evolution of  $\rho(\theta, \omega, t)$  degenerates to an invariant manifold, which is

$$\dot{a}(t) = i(K \sin \alpha - \omega) a(t) + \frac{1}{2} [H^*(t) - H(t) a^2(t)]. \quad (15)$$

Consequently, Eq. (15) is closed by the definition of the order parameter in Eq. (11), where

$$\begin{aligned} Z(t) &= \int_{-\infty}^{+\infty} g(\omega) a_{-1}(\omega, t) d\omega, \\ &= \int_{-\infty}^{+\infty} g(\omega) a^*(\omega, t) d\omega. \end{aligned} \quad (16)$$

We stress that Eq. (15) is still infinite dimensional because of the distributed natural frequencies. Thus, we may make a specific choice for the frequency distribution to get around this difficulty, e.g. a Lorentzian distribution  $g(\omega) = \Delta/[\pi(\omega - \mu)^2 + \Delta^2]$  with  $\Delta$  being the width of the distribution and  $\mu$  being the mean frequency. In this setting, the order parameters defined in Eq. (16) can be calculated by using Cauchy's residue theorem with analytical continuation of  $a(\omega, t)$  into the lower half complex plane, which leads to

$$Z(t) = a^*(\mu - i\Delta, t). \quad (17)$$

As a result, the low-dimensional evolution of the order parameter can be obtained by replacing  $\omega$  with  $\mu - i\Delta$  and by taking into account the complex conjugate, which reads

$$\dot{Z} = -\Delta Z + iZ(\mu - K \sin \alpha) + \frac{1}{2} [KZe^{i\alpha} - KZ^*Z^2e^{-i\alpha}]. \quad (18)$$

Rewrite above equation using polar coordinates  $Z(t) = R(t)e^{i\psi(t)}$ , we have

$$\dot{R} = \frac{R}{2} (K - 2\Delta - KR^2) \cos \alpha, \quad (19a)$$

$$\dot{\psi} = \mu + \frac{K}{2} (R^2 - 1) \sin \alpha. \quad (19b)$$

Obviously, the amplitude  $R(t)$  is decoupled from the mean phase  $\psi(t)$  and Eq. (19a) have a critical coupling strength  $K_c = 2\Delta$  and a pair of critical phase frustration  $|\alpha_c| = \pi/2$ . Let us first consider the simplest case of  $\Delta = 0, \mu = 0$ , which corresponds to the case of achiral particles. In this case, when  $|\alpha_c| > \pi/2$ , the system bifurcates to  $R = 0$ , which corresponds to the incoherent state in phase oscillators and lattice state in self-propelled particles, while for  $|\alpha_c| < \pi/2$ , the system has a unique stable fixed point at  $R = 1$ , which corresponds to the coherent state and swarming state, respectively.

For the incoherent state, the system is totally disordered with the phases distributed uniformly around the unit circle, i.e.,  $\rho(\theta, \omega, t) = g(\omega)/2\pi$ , which implies that the phase velocity of each oscillator/particle becomes

$$\dot{\theta}_i = \omega_i - K \sin \alpha. \quad (20)$$

Correspondingly, the rotational radii of  $i$ -th particle is

$$r_i = \frac{v}{\dot{\theta}_i} = \frac{v}{\omega_i - K \sin \alpha}. \quad (21)$$

## References

- [1] Michel Fruchart, Ryo Hanai, Peter B. Littlewood, and Vincenzo Vitelli. Non-reciprocal phase transitions. *Nature*, 592(7854):363–369, Apr 2021.
- [2] D. Levis, I. Pagonabarraga, and B. Liebchen. Activity induced synchronization: Mutual flocking and chiral self-sorting. *Phys. Rev. Res.*, 1:023026, Sep 2019.
- [3] Benno Liebchen and Demian Levis. Collective behavior of chiral active matter: Pattern formation and enhanced flocking. *Phys. Rev. Lett.*, 119:058002, Aug 2017.
- [4] Yichen Lu, Yixin Xu, Wanrou Cai, Zhuanghe Tian, Jie Xu, Simin Wang, Tong Zhu, Yali Liu, Mengchu Wang, Yilin Zhou, Chengxu Yan, Chenlu Li, and Zhigang Zheng. Self-organized circling, clustering and swarming in populations of chiral swarmalators. *Chaos, Solitons & Fractals*, 191:115794, 2025.

- [5] Edward Ott and Thomas M. Antonsen. Low dimensional behavior of large systems of globally coupled oscillators. *Chaos: An Interdisciplinary Journal of Nonlinear Science*, 18(3):037113, 09 2008.
- [6] Edward Ott and Thomas M. Antonsen. Long time evolution of phase oscillator systems. *Chaos: An Interdisciplinary Journal of Nonlinear Science*, 19(2):023117, 05 2009.
- [7] Bruno Ventejou, Hugues Chaté, Raul Montagne, and Xia-qing Shi. Susceptibility of orientationally ordered active matter to chirality disorder. *Phys. Rev. Lett.*, 127:238001, Nov 2021.
- [8] Yujia Wang, Bruno Ventéjou, Hugues Chaté, and Xia-qing Shi. Condensation and synchronization in aligning chiral active matter. *Phys. Rev. Lett.*, 133:258302, Dec 2024.